Biochemical and Biophysical Research Communications 460 (2015) 964–970

Contents lists available at ScienceDirect

Biochemical and Biophysical Research Communications

journal homepage: www.elsevier.com/locate/ybbrc

Crystal structure of CagL from *Helicobacter pylori* K74 strain

Jin Myung Choi [a, 1], Yun Hui Choi [c, 1], Muddenahalli Srinivasa Sudhanva [b], Sundaravinayagam Devakumar [b], Kun Ho Lee [d], Jeong-Heon Cha [c, **], Sung Haeng Lee [a, *]

[a] Department of Cellular and Molecular Medicine, Chosun University School of Medicine, Gwangju 501-759, Republic of Korea
[b] Department of Bio-Materials, Graduate School, Chosun University, Gwangju 501-759, Republic of Korea
[c] Department of Applied Life Science, The Graduate School, BK21 PLUS Project, Yonsei University College of Dentistry, Seoul 120-752, Republic of Korea
[d] Department of Biomedical Sciences, College of Natural Sciences, Gwangju 501-759, Republic of Korea

ARTICLE INFO

Article history:
Received 16 March 2015
Available online 1 April 2015

Keywords:
Protein structure
Helicobacter pylori
T4SS
CagL
RGD domain

ABSTRACT

Helicobacter pylori (Hp) CagL is a component of the type IV secretion system (T4SS) and interacts with integrin in host cells through its flexible RGD domain to translocate CagA. Differences in CagL amino acid polymorphisms between Western and East-Asian *Hp*s are correlated with clinical outcome. CagL of East-Asian clinical *Hp* isolate K74 ($CagL^{K74}$) contains multiple residue variations upstream of RGD motif and has different integrin binding affinities compared to those of CagL from Western *Hp* 26695. Here, we report the crystal structure of $CagL^{K74}$. The structure displayed a six-helix bundle including two short α-helices, and the RGD motif was found in the long rigid α2 helix flanked by the conserved protease-sensitive and RGD-helper sequences, as observed in $CagL^{26695}$. However, two additional salt bridges were found between the helices compared with the $CagL^{26695}$ structure, suggesting that the putative flexible region harboring the RGD motif may be more stable in this CagL variant.

1. Introduction

Helicobacter pylori (*Hp*) is a spiral-shaped gram-negative microaerophilic bacterium [1] and a human pathogen found in the stomach and upper gastrointestinal tract of >50% of the world's population [2]. People infected with *Hp* have an increased risk of developing gastric diseases, including peptic ulcers, gastric adenocarcinoma, and gastric lymphoma [1,3,4]. Consequently, *Hp* has been classified as a human class I carcinogen, such as the World Health Organization and International Agency for Research on Cancer [5]. East-Asian type *Hp* has a highly divergent cag pathogenicity island (cagPAI) with a significantly greater effect on cell growth when infected [6], suggesting that the cagPAI variation from East-Asian *Hp* may have an important role in the pathogenesis of *Hp*-mediated gastric cancer.

Hp cagPAI is associated with diseases that induce epithelial cells to secrete chemokines, such as interleukin-8 [7,8]. The hallmark of the secretion onset is the translocation of CagA oncoprotein from cagPAI positive *Hp* into epithelial cells, which is mediated by type IV secretion system (T4SS) [9]. The T4SS likely assembles a large complex of 27 cagPAI-encoded proteins, including CagL, CagY, CagH, CagT, CagX, and CagI [10]. However, the ultrastructure of the complex is unknown, and the interactions between components need to be clarified.

The *Hp* T4SS system has been suggested to interact with receptors on host cell surface to deliver the CagA oncoprotein [11], which may be mediated by the CagL protein of the T4SS complex [12]. The host cell counterparts that interact with CagL are heterodimeric integrin molecules, including α5β1, αVβ3 and αVβ5, in which the CagL RGD motif is responsible for the recognition [12,13]. The RGD (Arg-Gly-Asp) tripeptide, which is located in the fibronectin flexible loop, was originally identified as the sequence that interacts with many of the cell-surface receptors responsible for cell adhesion, migration, and survival, including integrins [14].

Recently, Widemann et al. reported that RGD motif and its surrounding CagL sequences enhance interactions with integrins to translocate CagA and upregulate gastrin expression on gastric epithelial cells [13], resulting in hypergastrinanemia and gastric adenocarcinoma. Further importance of CagL RGD-mediated integrin binding was reported using a cyclic RGD peptide, which interferes with binding of *Hp* CagL to integrins, such as αVβ3 [15]. These observations suggest that CagL protein resides on the front

* Corresponding author.
** Corresponding author.
E-mail addresses: jcha@yuhs.ac (J.-H. Cha), sunglee@chosun.ac.kr (S.H. Lee).
[1] These authors contributed equally to this work.

http://dx.doi.org/10.1016/j.bbrc.2015.03.135
0006-291X/

line in the interactions with the integrin receptors *via* the RGD sequence during *Hp*-related gastric carcinogenesis. However, RGD-dependent binding of CagL to integrin has been questioned, as CagA lacking an RGD sequence can interact with α5β1 [16]. Therefore, the CagL protein structure need to be determined to understand the molecular details of interactions with receptors and other components in the T4SS complex, such as CagI and CagH, considering the pathogenicity of *Hp* and the role of CagL in infection. In addition, determining the protein structure will help in the development of therapeutic drugs to prevent *Hp*s-host cell interactions.

In this study, we compared East-Asian *cagL* genes available in genome database with Western *cag*L from *Hp* 26695 consensus sequences, and chose CagL from K74 strain to determine structure. Multiple amino acids replacements were found in $CagL^{K74}$, particularly upstream of RGD motif, and the integrin binding capacity was examined. With subtle modifications of culture media components and expression host strain, we successfully obtained $CagL^{K74}$ protein in soluble form, which provided more advantage compared to the mutated and refolded CagL from *Hp* 26695 ($CagL^{26695}$) [17] for crystallization and biochemical studies. Subsequently, crystal structure of $CagL^{K74}$ was determined and compared to that of $CagL^{26695}$. Our results will provide a structural basis for comparative studies of various CagL orthologs from *Hp* strains.

2. Materials and methods

2.1. Gene cloning, protein expression, and purification

Hp 26695 and K74 were obtained from D. Scott Marrell and J. Cha, respectively, and full-length *cagL* genes were cloned and sequenced. The K74 *cagL* fragment (NCBI accession number: KP271158) encoding from E21 to K237 was subsequently cloned into pET28a (+) with N-terminal hexa-His tag, resulting in the exclusion of signal peptide. $CagL^{K74}$ mutants were created using a Muta-Direct Site-Directed Mutagenesis Kit (iNtRON biotechnology, Korea).

Native ($CagL^{K74}$ and $CagL^{26695}$) and Selenomethionine (Se-Met)-substituted $CagL^{K74}$ proteins were overexpressed in Rosetta2 (DE3) in the presence of 1 mM IPTG and 1% MetOH at 20 °C. The Se-Met $CagL^{K74}$ protein was produced in simplified culture conditions [18], in which cells were grown in minimal media containing 50 mg L-Se-Met/L. The proteins were enriched to homogeneity using Ni-affinity chromatography followed by Hi-Load 16/60 Superdex 200 gel filtration. The N-terminal 6 × His tag was cleaved with thrombin and removed during size exclusion chromatography (SEC).

2.2. Crystallization and data collection

Both native and Se-Met-substituted $CagL^{K74}$ were concentrated to 10 mg/ml in 20 mM Tris–HCl pH 7.5 and 50 mM NaCl for crystallization. Both proteins were crystallized by hanging drop method within 3–4 days in the same reservoir solution containing 0.1M Na-citrate pH 5.6, 10% iso-propanol, and 10% PEG 4000. Addition of 3% dioxane changed the crystal quality in size and shape, resulting in the diffraction to 2.8 Å and 2.9 Å for native and Se-Met CagL, respectively. The diffraction data were collected on beamline PAL-5C at the Pohang Light Source (PLS, South Korea) and were processed by HKL2000.

2.3. Structural determination and refinement

The structure of Se-Met-substituted $CagL^{K74}$ was determined using single-wavelength anomalous dispersion (SAD) method at a resolution of 2.9 Å. The positions of six selenium atoms (three Se-Met per CagL monomer in the asymmetric unit) were determined using AutoSol in PHENIX suit [19]. Subsequently, phases were calculated and an initial CagL model was built with AutoBuild program in the PHENIX suit. After several rounds of model building and refinement iterations, the Se-Met CagL structure was used as a search model to obtain phase information for the native dataset by molecular replacement using CCP4i suit [20]. The native $CagL^{K74}$ phases were continuously improved, and the resulting atomic model was refined to R_{work}/R_{free} of 20.12%/25.26% (Table 1). Atomic structure model building and refinement were performed with the Coot [21] and PHENIX, respectively.

2.4. Analytical size exclusion

Analytical SEC was carried out using HiLoad 16/60 Superdex 200 column. The SEC column was pre-equilibrated with a buffer containing 50 mM phosphate pH 7.2 and 150 mM NaCl. Purified $CagL^{K74}$ in 0.5 ml (2 mg) was passed through the column at a flow rate of 1 ml/min. A mixture of standard proteins (1.5–2 mg/protein in 0.5 ml) were prepared using LMW kit (GE healthcare, UK) and immediately passed through the column to generate a standard curve. The calibration curve was obtained based on the correlation between the retention times and molecular weights of known protein markers. The molecular weight of CagL in solution was estimated based on the calibration curve. Stokes radius (R_H) of $CagL^{K74}$ was estimated using the Stokes radii of known standard proteins and calculated from Protein Data Bank (PDB) structures using program the HYDROPRO ver.10 program [22].

2.5. Spot blotting assay

Interactions between the CagLs and integrins were detected using a spot blotting assay (Supplementary Method). In brief, proteins including the CagL proteins were spotted on a nitrocellulose membrane and incubated with each purified α5β1, αVβ3, or αVβ5 integrins (Chemicon-Millipore, USA). Chemiluminescence was used with specific antibodies to detect the integrins and monitor the interactions.

2.6. Sedimentation equilibrium analytical ultracentrifugation

A 24 μM CagL sample was prepared in 20 mM Tris-Cl pH 7.5 and 50 mM NaCl. Sedimentation equilibrium experiments were performed at 4 °C with a Beckman XL-A ultracentrifuge using an AN-60Ti two-hole rotor, and absorbance scans were taken at 25,000 rpm for 72 h. Data were analyzed using SEDPHAT software (http://www.analyticalultracentrifugation.com).

3. Results

3.1. CagL polymorphisms in Korean clinical Hps isolates

The *Hp* K74 *cagL* gene was sequenced and compared to *cagL* sequences of twelve registered East-Asian *Hp*s. The deduced amino acid sequences showed approximately 94.9% identities to those of East-Asian *Hp*s (Fig. S1). The CagL sequence comparison also revealed that K74 had the most amino acid variations compared with those of Western strain 26695, in which 10 amino acids were changed at positions of 35, 58, 59, 60, 62, 122, 201, 210, 216, and 234 (Fig. 1A). Interestingly, five (K35, D58, K59, I60, and K62) of the 10 $CagL^{K74}$ mutations were located upstream of the RGD motif, which is an important integrin binding region [23]. Furthermore, four of the five mutations in this region were drastic changes, such as Q35K, N58D, E59K, and E62K. Therefore, we chose $CagL^{K74}$ among the Korean clinical isolates for functional and structural studies.

Table 1
Data collection and refinement statistics of CagL$^{K.74}$.

	Se-Met_CagL	Native_CagL
Diffraction statistics		
Beam line	PAL-5CPAL-5C	
Wavelength (Å)	0.97943	0.97938
Space group	$P4_32_12$	$P4_32_12$
Cell parameters		
a, *b*, *c* (Å)	97.761, 97.761, 144.838	97.616, 97.616, 144.242
α, *β*, γ (°)	90.0, 90.0, 90.0	90.0, 90.0, 90.0
Data resolution (Å)	50.0-2.9 (2.95-2.90)	50.0-2.8 (2.9-2.8)
Completeness (%)	100	98.5 (94.6)
Redundancy	15.0 (13.1)	6.0 (3.5)
Total reflection	243436	106426
Unique reflections	16234 (775)	17703 (1639)
R-merge[a] (%)	22.9 (33.7)	11 (33)
Average I/σ	5.4 (3.5)	14 (2.6)
Matthew's coefficient (Å^3 Da^{-1})	2.36	2.32
Solvent content (%)	48	46.95
Refinement		
R_{work}/R_{free} (%)		20.12/25.67
Protein residues/water		410/82
RMSD		
Angle (°)		1.072
Length (Å)		0.009
Average B-factors (Å^2)		19.75
Ramachandran plot		
Most favored regions (%)		95.29
Allowed regions (%)		4.47
Outliers (%)		0.25

Values in parentheses correspond to highest resolution shell.
[a] R-merge = $\sum_{hkl} \sum_i |I_i(hkl) - < I(hkl) >| / \sum_{hkl} \sum_i I_i(hkl)$, where $I_i(hkl)$ is the observed intensity and $<I(hkl)>$ is the average intensity of symmetry-related observations.

Cloned CagL^{K74} was overexpressed in the soluble fraction and purified in enough amounts for crystallization trials (Fig. 1B), whereas CagL^{26695} was obtained by refolding the inclusion body, and was mutated to reduce high entropy fractions of the refolded proteins [17,23]. Thus, CagL^{K74} was closer to the native form of protein, as it was free from the modifications and refolding. The spot blotting assay demonstrated the binding abilities of CagL^{K74} and CagL^{26695} with each of the purified integrins (α5β1, αVβ3, and αVβ5; Fig. 1C). Interestingly, the binding abilities of CagL^{K74} were significantly higher than those of CagL^{26695}.

3.2. Overall structure of CagL^{K74}

We crystallized both *Hp* K74 native and Se-Met CagL. Both crystals belonged to the $P4_32_12$ space group (Table 1) and contained two molecules in asymmetric unit. In the final model, all residues in each molecule were defined, except three the N-terminus residues (21–23), four loop1 (L1) residues (52–55) connecting α1 to α2, and six C-terminus residues (232–237) (Fig. 1D). Two molecules in the asymmetric unit were associated with the anti-parallel helix interaction forming a two-2-fold non-crystallographic symmetry, and were structurally similar with an RMSD value of 0.59 in Cα (Fig. 1D). The CagL^{K74} monomer was folded in an elongated bundle consisting of four long helices (α1, α2, α5, and α6) and two short helices (α3 and α4) (Fig. 2). Among the CagL^{K74} interactions, two short helices (α3 and α4) were likely stabilized by the following bond formations (Fig. 2). First, a disulfide bond between C128 and C139 bridged helix 5 to the C-terminus of the short α4. Second, Y103 in short α3 formed π-π interaction with Y113 in the C-terminal of α2, and the amide nitrogen of L119 hydrogen bonded with E140 in α5.

The conserved residues residing in α2, α5, and α6 likely participated in maintaining the CagL architecture. As shown in Fig. 2, three salt bridges and one hydrogen bond were formed between helices 5 and 6 (D132 and R229, K149 and D212, K149 and E215 for salt bridges, and D132 and Y225 for H-bonds), and three hydrogen bonds were also found between α2 and α5 (N85 and S159, N89 and S159, D78 and N166). In addition to these interactions, the F86, F92, F93, F100, Y163, H200, F204, and Y207 side chains on helices of α2, α5, and α6 formed hydrophobic core, holding the three helices together by hydrophobic interaction (Fig. 2). Although CagL appeared to fold loosely, the shape of the protein was likely maintained by those intramolecular covalent and weak interactions among α2, α5, and α6. The role of the conserved residues seems to be common for maintaining the helix backbone, compared to that in the CagL^{26695} structure. In this regard, the α1 and α2 helices may be as flexible as those observed in CagL^{26695}, as evidenced by the lack of protein stability and cell adhesion [17]. This finding suggests that the role of the two helices in the host-*Hp* interaction is critical despite that the RGD motif (R76-D78) is located in the rigid α2 helix.

3.3. Assembly of CagL^{K74} in solution

Our crystal structure may indicate that dimer of CagL^{K74} is possibly the functional unit in cell since the number of molecules in asymmetric unit tends to correlate with oligomeric state in solution. Protein interactions occurred in the α5-α6 interface that buried an accessible surface area of 1629.2 Å^2 through various bond types, including hydrogen bonds (T175-E219 and S177-R223), salt bridges (K187-Q220 and R194-E209), and hydrophobic interactions (L156-L160, L198-L205, and I190–I216) (Fig. S2). We systematically created combinations of mutants to abolish the interactions and separate the two potential dimers in solution (Table S1). SEC was performed to determine the molecular masses of CagL^{K74} and its mutants. To our surprise, the wild-type and all of the mutants had similar molecular masses of ~49.5 kD corresponding to that of a dimer (calculated monomer molecular mass of ~24.6 kD) (Fig. 3A and S3). However, whether the oligomeric state is actually a dimer remains to be answered, as CagL adopted an elongated structure.

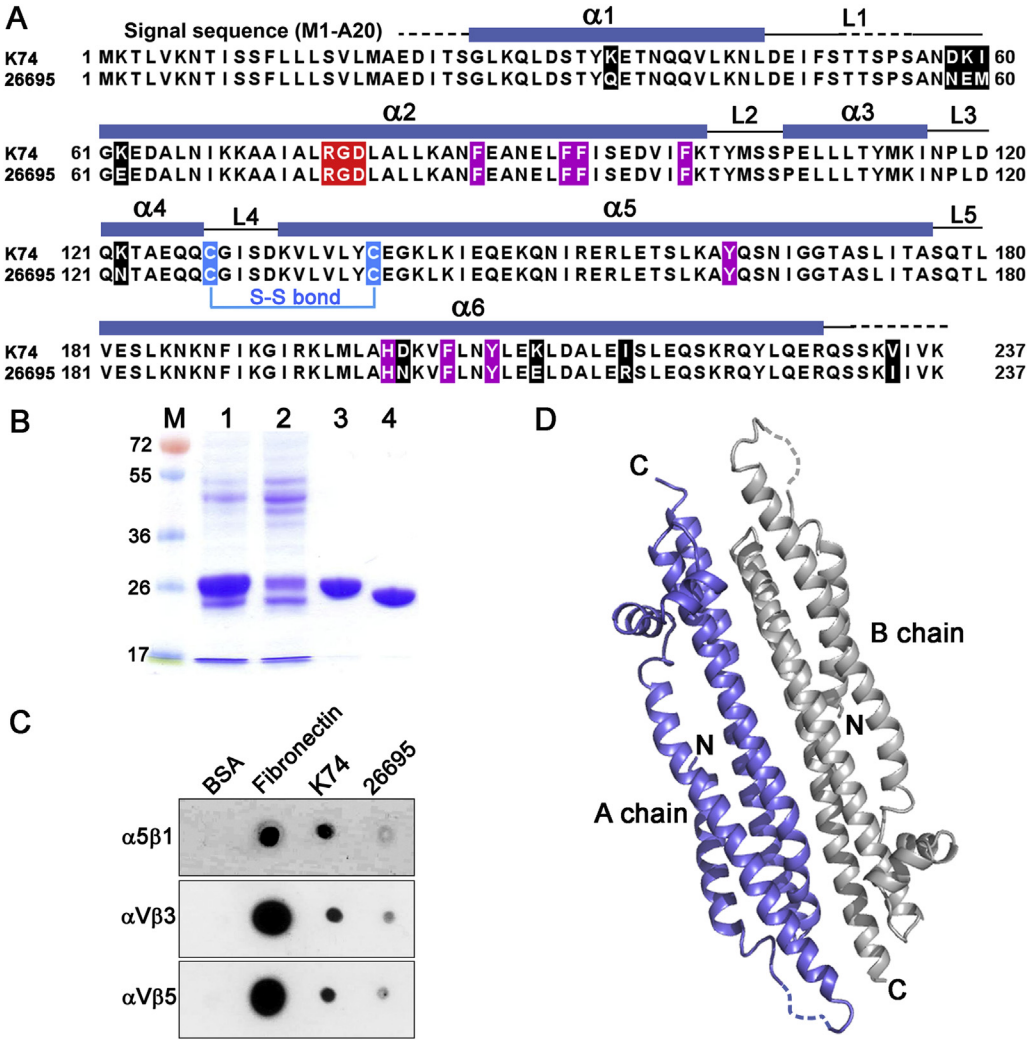

Fig. 1. Sequence alignment, purification, and CagL binding with integrins. (A) Sequence alignment of CagL^{K74} and CagL^{26695}. Secondary structure elements of CagL^{K74} are shown with the aligned sequence. Black dash lines are disordered regions. Variant residues on both CagL sequence (K74 and 26695) were highlighted in black, and hydrophobic residues and cysteine for disulfide bond were in magenta and in cyan, respectively. (B) CagL^{K74} was purified in soluble form and analyzed by 12% SDS-PAGE. lane 1, supernatant from induced cells; lane 2, unbound fraction from Ni-NTA agarose column; lane 3, 6XHis-tagged CagL^{K74}; lane 4, thrombin cleaved CagL^{K74}. (C) Spot blotting assay for the interaction between proteins containing RGD motif and integrins. BSA and fibronectin were used as negative and positive control, respectively. (D) Crystal structure of CagL in an asymmetric unit containing two chains in 2-fold NCS. The disordered regions were shown as dashed lines.

Therefore, we first estimated the CagL Stokes radius (R_H) based on the SEC with R_H values of known standard proteins. The CagL R_H value (2.9 nm) was greater than that of carbonic anhydrase (R_H: 2.3 nm, 29 kD), suggesting that CagL does not exist as a monomer or in a globular shape in solution (Fig. 3A). Thus, sedimentation equilibrium experiments were performed to determine the CagL^{K74} oligomeric state. The plot was best fit to the function of a single species the best, and data were converged to a monomeric model with a minimal deviation in the residuals (Fig. 3B), resulting in a molecular mass of 26.0 kD. These results suggest that the CagL functional unit in solution is very likely to be a monomer in an elongated shape.

3.4. Potential role of sequence variation in helix packing

The structure of the CagL^{26695} became available during this CagL^{K74} structural study. As shown in Fig. 1A, sequence identity between the two homologs was 96%. Furthermore, CagL^{K74} had a relatively low amino acid homology level of 27% with TraC, a CagL ortholog in the T4SS from *Agrobacterium tumefaciens* [24]. This clearly indicates that the two CagL crystal structures were very likely similar. Indeed, CagL^{K74} was superimposed on two *Hp* 26695 CagL structures (CagL^{26695Meth} and CagL^{26695KKQEK}) with an RMSD values of 1.39 and 3.30 in Cα (Fig. 4A), respectively, suggesting that our structure is physiologically closer to the native species in cell than CagL^{26695} structure that was modified to increase crystallization propensity. Note that five residues were replaced in CagL^{26695KKQEK} (K69A, K70T, Q147A, E148T, and K149A) and methyl groups were introduced into lysine residues in CagL^{26695meth} *in vitro* [17].

The structural comparison indicated that these two CagLs (CagL^{K74} and CagL^{26695}) share architectural similarities important for biological function; both structures maintained a long α2 helix, on which the biologically important RGD motif was found (Fig. 4A). The CagL^{K74} structure also revealed a similar helical conformation of RGD motif with two strong salt bridge formations within adjacent helices. Notably, one of the amino acid variations in *Hp* CagL^{K74} created an additional interaction between α1 and α2. K35 (Q35 in 26695) in α1 provided two ionic bonds with E87 and E90 in α2 (Fig. 4B), suggesting that α1 helix in CagL^{K74} may be packed tighter with core helices than that in CagL^{26695}. Besides the extra bonds formation, additional

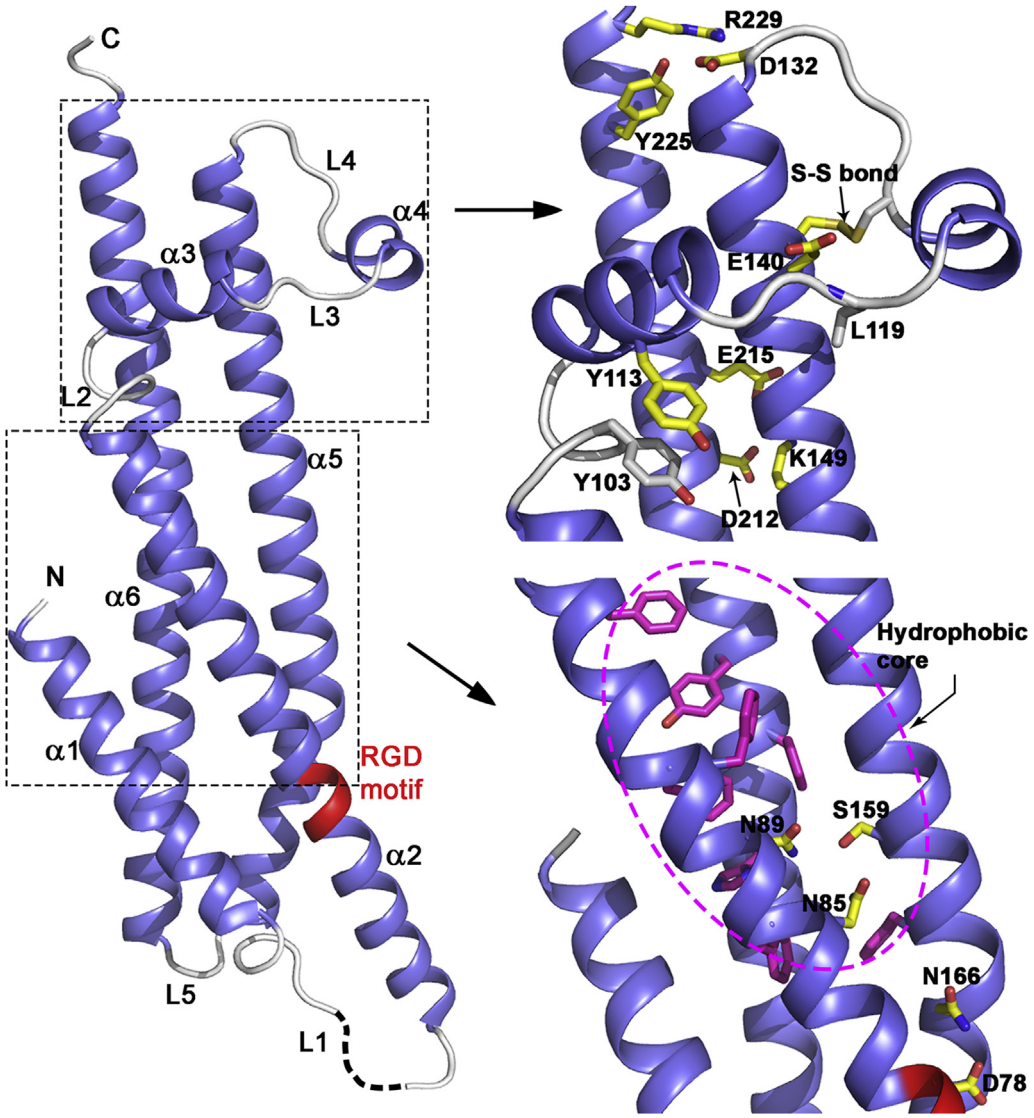

Fig. 2. Overall structure of CagL^{K74}. Monomer of CagL (chain A) consists of six helices. The two important regions for CagL architecture were boxed (left) and the interaction of residues between helices shown as stick (upper right). Hydrophobic core region was shown as dashed circle (lower right).

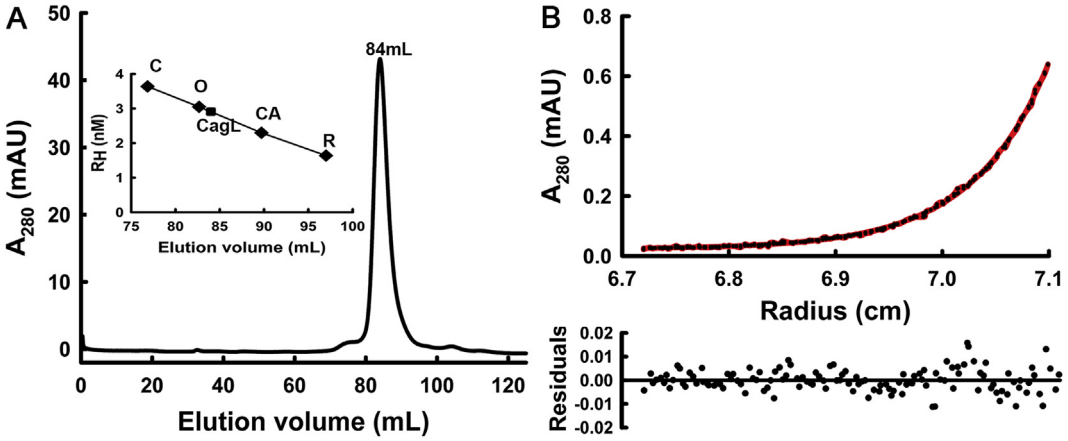

Fig. 3. Oligomeric state of CagL^{K74}. (A) CagL was monitored to high peak region (84 mL) during SEC. R_H of CagL (■) was measured to 2.91 nm from graph of stokes radius (R_H) *vs* elution volume with standard proteins (◆) including conalbumin (R_H = 3.64 nm, 75.0 kD, 76.8 mL), Ovalbumin (R_H = 3.05 nm, 44.0 kD, 82.7 mL), carbonic anhydrase (R_H = 2.30 nm, 29.0 kD, 89.7 mL), ribonuclease A (R_H = 1.64, 13.7 kD, 97.0 mL); (B) Equilibrium sedimentation analytical ultracentrifugation (AUC) of CagL. Spots represent experimental data and the fitting line is in red for monomer. (For interpretation of the references to colour in this figure legend, the reader is referred to the web version of this article.)

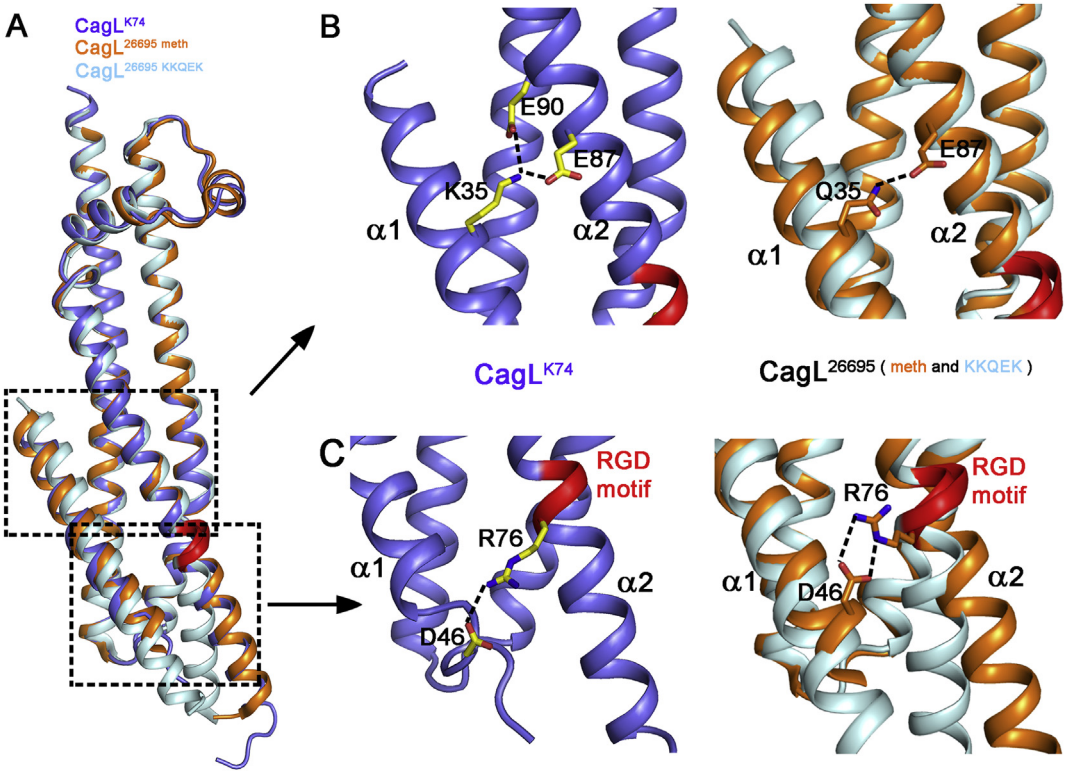

Fig. 4. Structural comparison between CagL^{K74} and CagL^{26695}. (A) Cartoon representation of CagL^{K74} (slate), CagL^{26695meth} (orange) and CagL^{26695KKQEK} (palecyan) by superimposition. Regions that involves in the additional bonds formation in CagL^{K74} between helices are pointed in boxes. (B) K35 of α1 in CagL^{K74} forms salt bridges with E87 and E90 (left) but Q35 of α1 in CagL^{26695meth} only interacts with E87 (right). (C) Interaction between D46 on α1 and R76 of RGD motif on α2 in CagL^{26695} and CagL^{K74} is shown. While D46 of CagL^{26695} found on helix, D46 in CagL^{K74} resides on loop, which may stabilize the loop *via* electrostatic interaction with R76. In both (B) and (C), those side chains were shown for CagL^{K74} (yellow) and CagL^{26695meth} (orange). No such interaction was formed in CagL^{26695KKQEK}, resulting.in the flexible α2 helix. (For interpretation of the references to colour in this figure legend, the reader is referred to the web version of this article.)

variations also occurred in the proximal end of the L1 at amino acid numbers D58, K59, I60, and K62. However, these amino acids were not involved in loop flexibility due to a lack of significant inter-loop interactions.

4. Discussion

We have determined the crystal structure of CagL from *Hp* K74 strain and demonstrated the structural differences in CagLs. The anti-paralleled dimeric association of CagL^{K74} in the asymmetric unit may not be reconciled with oligomeric status in solution. The CagL functional unit in solution is likely to be a monomer, considering the estimated Stokes radius and molecular weight from analytical ultracentrifugation. Certainly, the expected oligomeric state correlated with the calculated R_H values (2.58 nm for the monomer and 2.78 nm for the dimer) based on our CagL^{K74} crystal structure.

Although the structures of the two CagLs (CagL ^{K74} and ^{26695}) were similar as shown at Fig. 4A, sequence polymorphisms in conjunction with structures may provide insight into the biological functions of CagL during T4SS-mediated interactions with host cell. It has been believed that the RGD sequence adopts a partly flexible and loopy structure [15], which, in turn, is suitable to interact with integrin on the target cell membrane [14]. However, the CagL RGD sequence was found on the long rigid α2 helix in both CagL structures. Therefore, the unprecedented location of the RGD in the rigid helix 2 on both CagL structures raises the question whether the motif or protein itself is involved in the direct contact with host cell or whether another part of the protein could be responsible for the interaction. As both questions are tightly associated with the nature of the RGD sequence, plasticity of the α1 and α2 helices is also important. Previous research has suggested that the loose interactions of α1 helix with adjacent helices including α2 could result in bending of α2 and subsequent local unwinding around RGD sequence [17]. As shown in the CagL^{K74} structure, an additional salt bridge by K35 likely tightens the interaction between α1 and α2. Furthermore, D46 in CagL^{K74}, which forms a salt bridge with R76 in RGD resides in the loop, whereas the D46 in CagL^{26695} was found in the α1 helix (Fig. 4C). This observation agrees with the finding that our protein was comparatively more stable against long-term storage than that of refolded CagL^{26695}, which was auto-degradable and protease sensitive in the same region [17]. These observations may indicate that the two helices in CagL^{K74} are packed tighter and less flexible around the RGD motif than those of the region of CagL^{26695}. Thus, the RGD motif is likely to remain rigid and may not be the main sequence for the CagL-host cell membrane interaction. The complex structure of talin with integrin suggested that a non-RGD sequence participates in the interaction, as the talin F2–F3 domain interface does not contain an RGD sequence [25]. In addition, RGD-independent translocation of CagA into host cells by T4SS indicates that CagL may not be a necessary component for host-pathogen recognition [16]. Therefore, another region of the protein may be involved in the integrin interaction. Indeed, mutations on loops in our preliminary studies impaired the translocation of CagA, whereas RGD to AAA mutations resulted in the translocation of CagA (data not shown). The CagL structure with respect to host interaction *via* RGD sequence remains unclear. The complex structure of CagL with integrin needs to be determined to

elucidate the precise role of the canonical RGD motif in T4SS-mediated *Hp* carcinogenesis.

Conflict of interest

None.

Acknowledgments

This work was supported in part by research funds from Chosun University (2008) and NRF-2013R1A1A2057465 to S.H.Lee, NRF-2012R1A1A2008554 to J.H.Cha, and 2011-0017009 from Korea Research Foundation to K.H.Lee. We thank Dr. Young Jun Im for critics to this manuscript and the beamline (PLS-5C) staffs at Pohang Light Source for technical support during data collection.

Appendix A.. Supplementary data

Supplementary data related to this article can be found at http://dx.doi.org/10.1016/j.bbrc.2015.03.135.

Transparency document

Transparency document related to this article can be found online at http://dx.doi.org/10.1016/j.bbrc.2015.03.135.

References

[1] G.E. Buck, *Campylobacter pylori* and gastroduodenal disease, Clin. Microbiol. Rev. 3 (1990) 1–12.
[2] L.M. Brown, *Helicobacter pylori*: epidemiology and routes of transmission, Epidemiol. Rev. 22 (2000) 283–297.
[3] M.R. Amieva, E.M. El-Omar, Host-bacterial interactions in Helicobacter pylori infection, Gastroenterology 134 (2008) 306–323.
[4] Interesting Insights into Authors' Minds 23, 2009, p. 15. Access (10300155).
[5] R. Pandey, V. Misra, S.P. Misra, M. Dwivedi, A. Kumar, B.K. Tiwari, Helicobacter pylori and gastric cancer, Asian Pac J. Cancer Prev. 11 (2010) 583–588.
[6] H.Y. Fu, K. Asahi, Y. Hayashi, H. Eguchi, H. Murata, M. Tsujii, S. Tsuji, T. Azuma, S. Kawano, East Asian-type Helicobacter pylori cytotoxin-associated gene A protein has a more significant effect on growth of rat gastric mucosal cells than the western type, J. Gastroenterol. Hepatol. 22 (2007) 355–362.
[7] S. Odenbreit, J. Puls, B. Sedlmaier, E. Gerland, W. Fischer, R. Haas, Translocation of Helicobacter pylori CagA into gastric epithelial cells by type IV secretion, Science 287 (2000) 1497–1500.
[8] G. Rieder, R.A. Hatz, A.P. Moran, A. Walz, M. Stolte, G. Enders, Role of adherence in interleukin-8 induction in Helicobacter pylori-associated gastritis, Infect. Immun. 65 (1997) 3622–3630.
[9] R. Fronzes, P.J. Christie, G. Waksman, The structural biology of type IV secretion systems, Nat. Rev. Microbiol. 7 (2009) 703–714.
[10] S. Backert, R. Fronzes, G. Waksman, VirB2 and VirB5 proteins: specialized adhesins in bacterial type-IV secretion systems? Trends Microbiol. 16 (2008) 409–413.
[11] N.S. Akopyants, S.W. Clifton, D. Kersulyte, J.E. Crabtree, B.E. Youree, C.A. Reece, N.O. Bukanov, E.S. Drazek, B.A. Roe, D.E. Berg, Analyses of the cag pathogenicity island of Helicobacter pylori, Mol. Microbiol. 28 (1998) 37–53.
[12] T. Kwok, D. Zabler, S. Urman, M. Rohde, R. Hartig, S. Wessler, R. Misselwitz, J. Berger, N. Sewald, W. Konig, S. Backert, Helicobacter exploits integrin for type IV secretion and kinase activation, Nature 449 (2007) 862–866.
[13] T. Wiedemann, S. Hofbaur, N. Tegtmeyer, S. Huber, N. Sewald, S. Wessler, S. Backert, G. Rieder, Helicobacter pylori CagL dependent induction of gastrin expression via a novel alphavbeta5-integrin-integrin linked kinase signalling complex, Gut 61 (2012) 986–996.
[14] M.Z. Gilcrease, Integrin signaling in epithelial cells, Cancer Lett. 247 (2007) 1–25.
[15] J. Conradi, S. Huber, K. Gaus, F. Mertink, S. Royo Gracia, U. Strijowski, S. Backert, N. Sewald, Cyclic RGD peptides interfere with binding of the Helicobacter pylori protein CagL to integrins alphaVbeta3 and alpha5beta1, Amino Acids 43 (2012) 219–232.
[16] L.F. Jimenez-Soto, S. Kutter, X. Sewald, C. Ertl, E. Weiss, U. Kapp, M. Rohde, T. Pirch, K. Jung, S.F. Retta, L. Terradot, W. Fischer, R. Haas, Helicobacter pylori type IV secretion apparatus exploits beta1 integrin in a novel RGD-independent manner, PLoS Pathog. 5 (2009) e1000684.
[17] S. Barden, S. Lange, N. Tegtmeyer, J. Conradi, N. Sewald, S. Backert, H.H. Niemann, A helical RGD motif promoting cell adhesion: crystal structures of the Helicobacter pylori type IV secretion system pilus protein CagL, Structure 21 (2013) 1931–1941.
[18] S.A. Guerrero, H.J. Hecht, B. Hofmann, H. Biebl, M. Singh, Production of selenomethionine-labelled proteins using simplified culture conditions and generally applicable host/vector systems, Appl. Microbiol. Biotechnol. 56 (2001) 718–723.
[19] P.H. Zwart, P.V. Afonine, R.W. Grosse-Kunstleve, L.W. Hung, T.R. Ioerger, A.J. McCoy, E. McKee, N.W. Moriarty, R.J. Read, J.C. Sacchettini, N.K. Sauter, L.C. Storoni, T.C. Terwilliger, P.D. Adams, Automated structure solution with the PHENIX suite, Methods Mol. Biol. 426 (2008) 419–435.
[20] G.N. Murshudov, P. Skubak, A.A. Lebedev, N.S. Pannu, R.A. Steiner, R.A. Nicholls, M.D. Winn, F. Long, A.A. Vagin, REFMAC5 for the refinement of macromolecular crystal structures, Acta Crystallogr. D. Biol. Crystallogr. 67 (2011) 355–367.
[21] P. Emsley, K. Cowtan, Coot: model-building tools for molecular graphics, acta crystallographica. Section D, Biol. Crystallogr. 60 (2004) 2126–2132.
[22] A. Ortega, D. Amoros, J. Garcia de la Torre, Prediction of hydrodynamic and other solution properties of rigid proteins from atomic- and residue-level models, Biophys. J. 101 (2011) 892–898.
[23] J. Conradi, N. Tegtmeyer, M. Wozna, M. Wissbrock, C. Michalek, C. Gagell, T.L. Cover, R. Frank, N. Sewald, S. Backert, An RGD helper sequence in CagL of Helicobacter pylori assists in interactions with integrins and injection of CagA, Front. Cell. Infect. Microbiol. 2 (2012) 70.
[24] H.J. Yeo, Q. Yuan, M.R. Beck, C. Baron, G. Waksman, Structural and functional characterization of the VirB5 protein from the type IV secretion system encoded by the conjugative plasmid pKM101, Proc. Natl. Acad. Sci. U S A 100 (2003) 15947–15952.
[25] N.J. Anthis, K.L. Wegener, F. Ye, C. Kim, B.T. Goult, E.D. Lowe, I. Vakonakis, N. Bate, D.R. Critchley, M.H. Ginsberg, I.D. Campbell, The structure of an integrin/talin complex reveals the basis of inside-out signal transduction, EMBO J. 28 (2009) 3623–3632.